SUPPLEMENTARY INFORMATIONS

Poly(ADP-ribose) controls DE-cadherin-dependent stem cell maintenance and oocyte localization

Yingbiao Ji and Alexei V. Tulin

This PDF file includes:

Supplementary Figures S1-S6

Supplementary Tables S1-S2

Supplementary Discussion

Supplementary Methods

Supplementary References

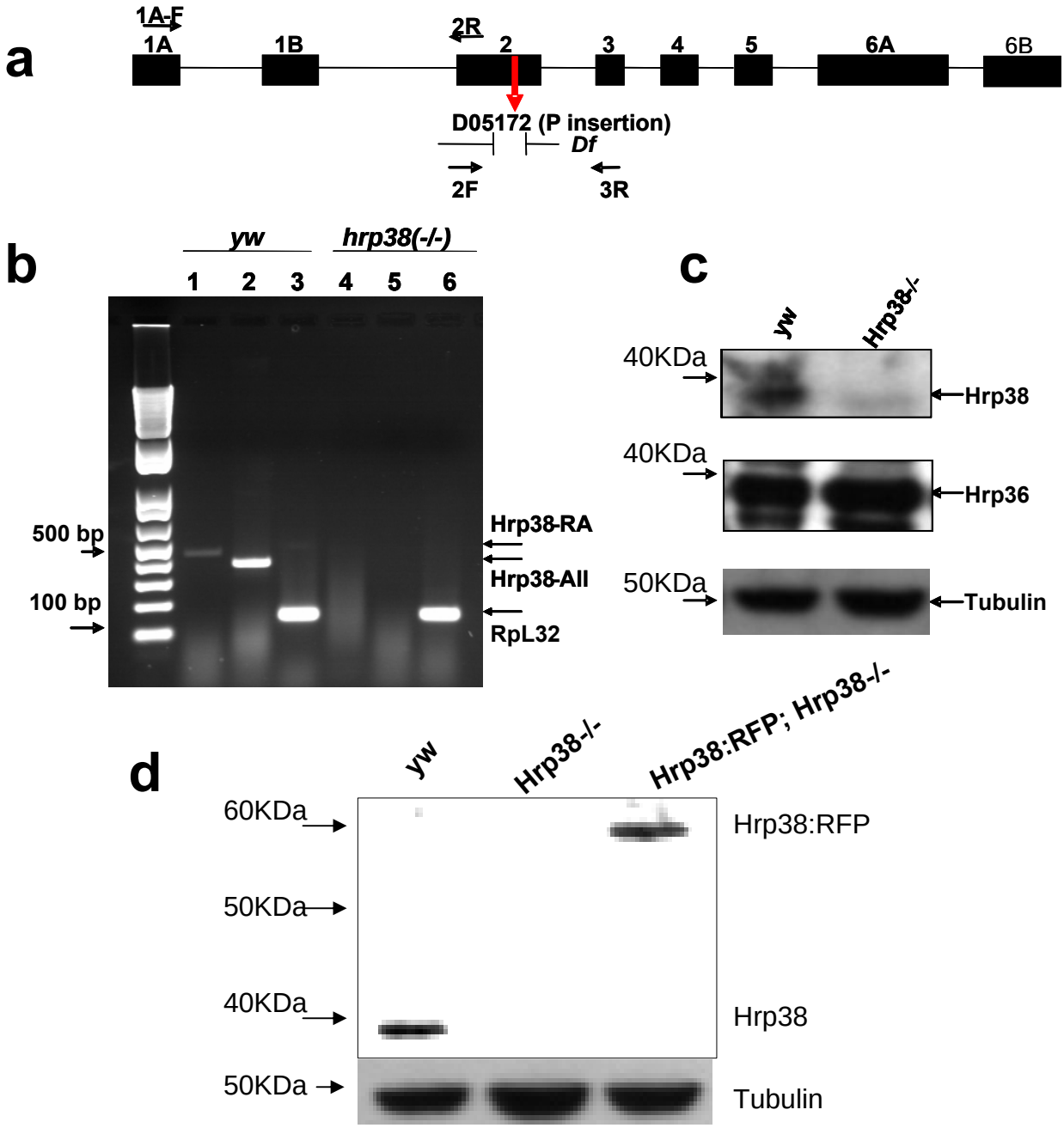

Supplementary Figure S1. ***Hrp38do5172*** **is a null mutation of the** ***hrp38*** **gene.** **(a)** The positions of P-element insertion (*P[XP]d05172*) and the deficiency (*Df(3R)Exel6209*) in the *hrp38* gene. **(b)** RT-PCR analysis of *hrp38* expression in the *hrp38* hemizygotes (*hrp38d05172/Df*) and wild-type (*y,w*) flies at the third-instar larvae stage. The wild-type flies have normal expression of hrp38-RA (lane 1) and hrp38-All (all transcripts, lane 2) transcripts. The *hrp38* hemizygotes did not express either hrp38-RA (lane 4) or hrp38-All (lane 5). *Rpl32* as the endogenous control in lane 3 and lane 6. The prime positions for hrp38-RA and hrp38-All were indicated in **(a)**. **(c)** Western blot analysis of Hrp38 expression in the *hrp38* hemizygotes (*hrp38d05172/Df*) and wild-type flies at the third-instar larvae stage. 50 µg total protein from the indicated genotypes was immunoblotted with rabbit anti-Hrp38 antibody (upper panel) and mouse anti-Hrp36 antibody (middle panel), respectively. In contrast to the wild type, the *hrp38* hemizygotes showed significantly lower expression of Hrp38, but not Hrp36, suggesting specificity of this antibody to Hrp38. The same blot in the upper panel was stripped and probed with mouse anti-Tubulin antibody in the lower panel. **(d)** Western blot analysis of Hrp38:RFP expression in the *hrp38* mutation (*hrp38d05172/Df*) background. The proteins from the adult flies of the wild type (*yw*), the *hrp38* mutant escapers (*hrp38d05172/Df*), and the rescued *hrp38* mutant (*pUAST-Hrp38:RFP/arm-Gal4; hrp38d05172/Df*) were immunoblotted with the anti-Hrp38 antibody (upper panel). A major 60 kDa Hrp38:RFP fusion protein was present in the rescued fly (*UAST-Hrp38:RFP/arm-Gal4; hrp38d05172/Df*) whose genotype was further verified by the absence of endogenous *hrp38* expression.

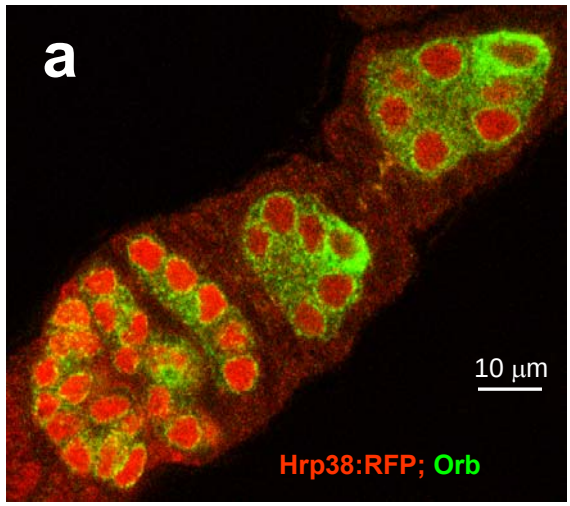

UASp:hrp38-RFP/Nos-GAL4; Hrp38-/Df

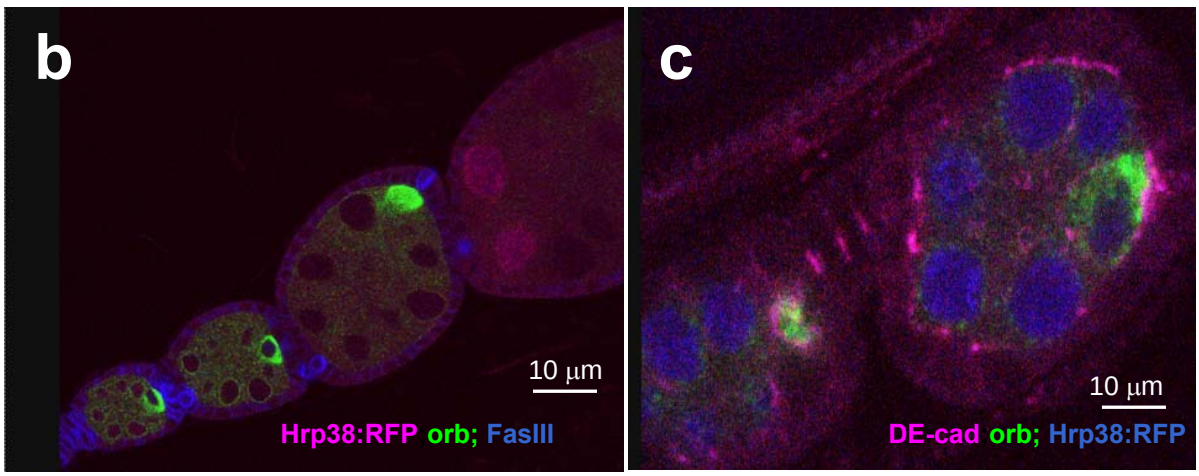

UASp:hrp38-RFP/Nos-GAL4; Hrp38-/Df

Supplementary Figure S2. Expression of Hrp38:RFP in the germline cells fully rescued the phenotypes shown in the *hrp38* mutant. (a) The normal oocyte localization in the *hrp38* mutant with expression of Hrp38:RFP in the germline cells. Orb staining for labeling the oocyte. **(b)** The normal specification of polar cells in the *hrp38* mutant with expression of Hrp38:RFP in the germline cells. The polar cells are labeled by FasIII staining. **(c)** The normal DE-cadherin expression pattern for positioning the oocyte in the posterior pole in the *hrp38* mutant with expression of Hrp38:RFP in the germline cells. In **(a-c)** the anterior pole of all egg chambers is to the left; the posterior pole is to the right.

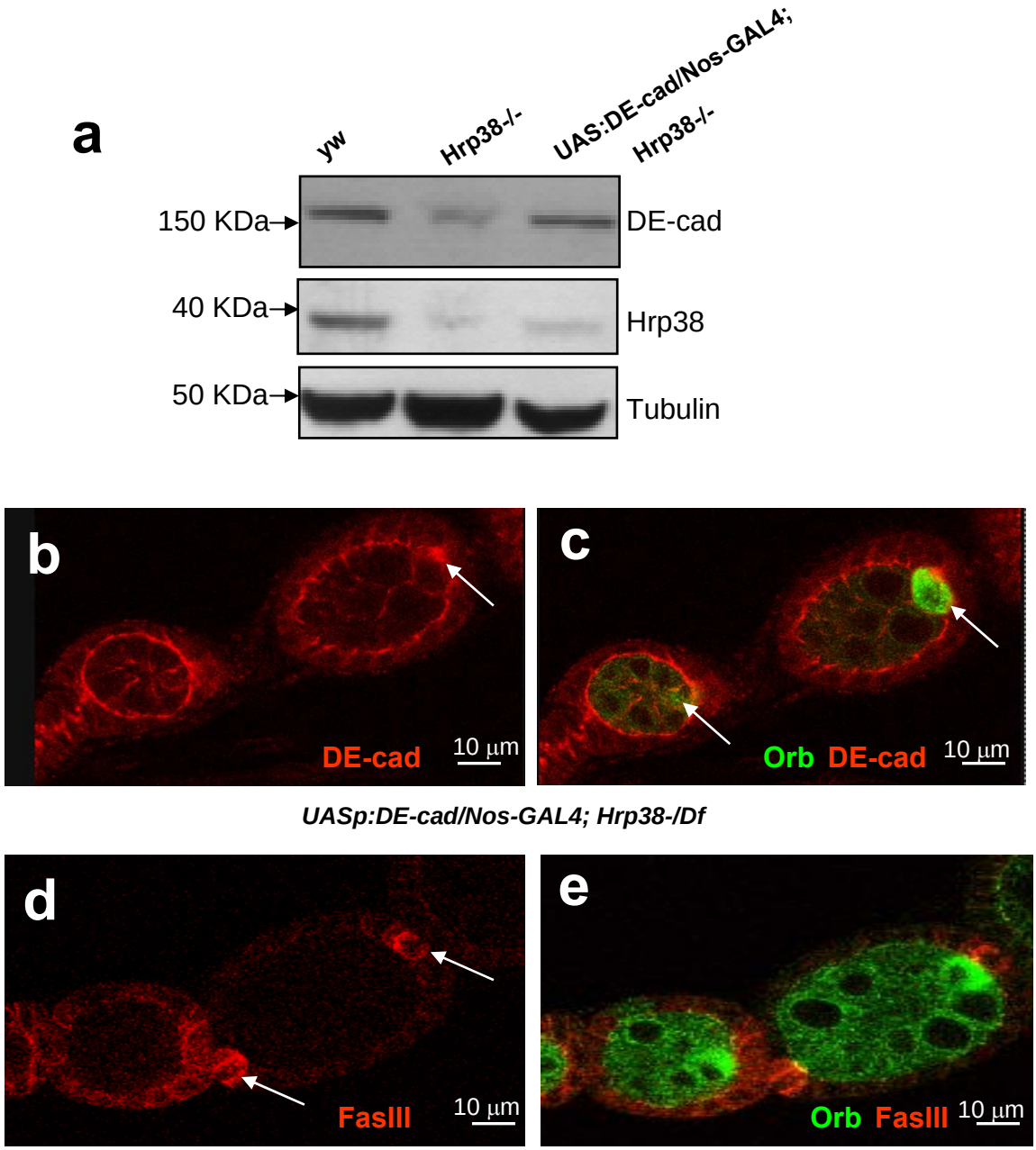

Supplementary Figure S3. Expression of DE-cadherin transgene in the germline cells fully rescued the oocyte mislocalization phenotype shown by the *hrp38* mutant. (a) Western blot analysis of UASp:DE-cadherin expression in the ovary in the *hrp38* mutation (*hrp38d05172/Df*) background. Equal amounts of ovary proteins from the wild-type fly (*y,w*), the *hrp38* mutant (*hrp38d05172/Df*) and the genotype (*pUASp>DE-cadherin/Nos-Gal4; hrp38d05172/Df*) were immunoblotted with anti-DE-cadherin (upper panel), anti-Hrp38 (middle panel) and anti-Tubulin (loading control, lower panel) antibodies, respectively. DE-cadherin expression in the genotype (*pUASp:DE-cadherin/Nos-Gal4; hrp38d05172/Df*) was restored to the normal expression level comparable to that of the wild-type fly (*y,w*). **(b,c)** The elevated DE-cadherin expression in the posterior pole (**b**, arrow indicated) and normal oocyte localization (**c**, arrows indicated) in the egg chambers of the *hrp38* mutant with expression of DE-cadherin in the germline cells. **(d,e)** Normal specification of polar cells in the *hrp38* mutant with expression of DE-cadherin in the germline cells. The polar cells are labeled by FasIII staining (arrow in **d**). **(c,e)** The oocyte was labeled by Orb staining. The anterior pole of all egg chambers is to the left, and the posterior pole is to the right. All scale bars represent 10 μm.

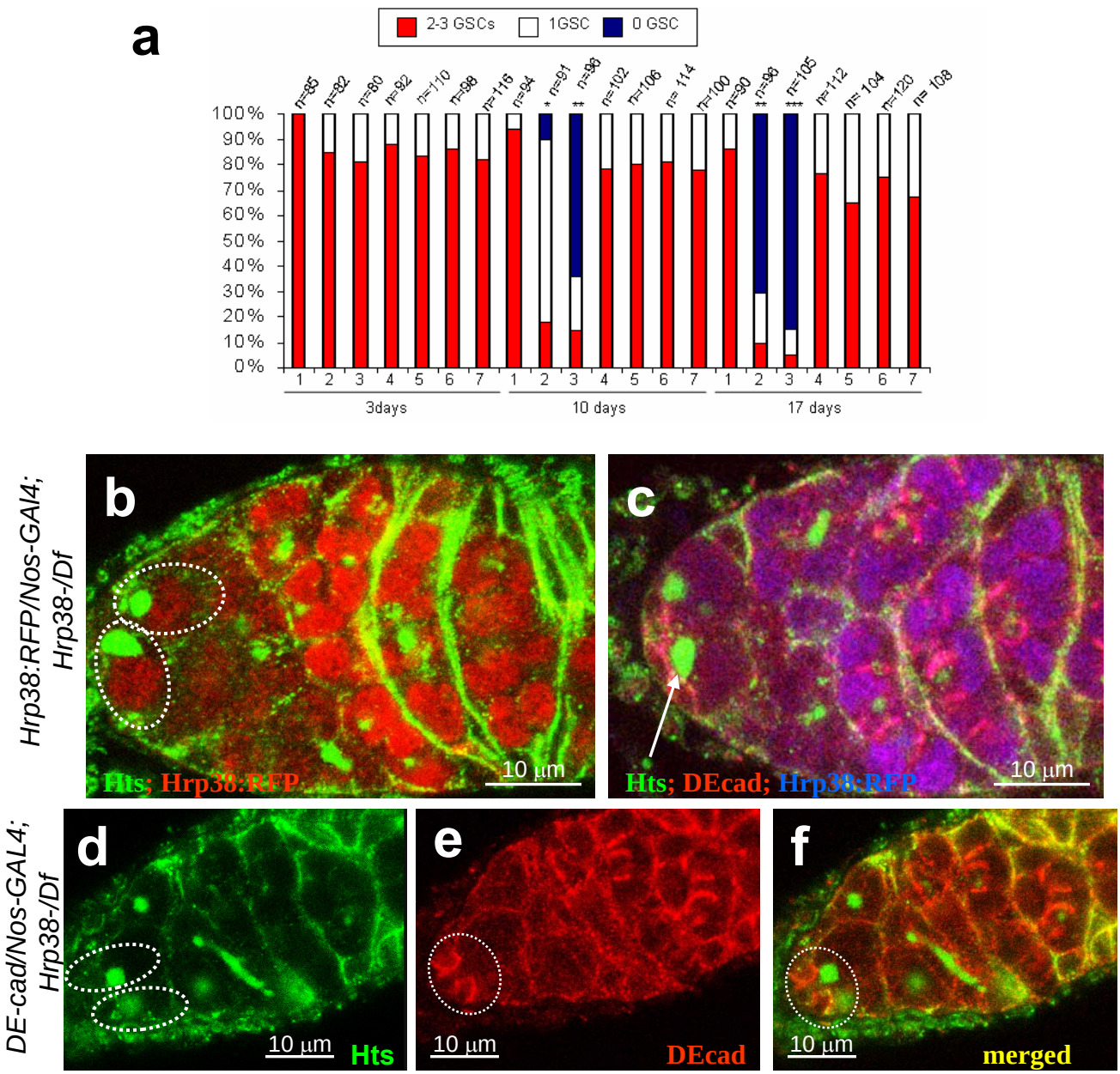

Supplementary Figure S4. Expression of Hrp38:RFP and DE-cadherin transgene in the germline cells rescued GSC self-renewal ability of the *hrp38* mutant. (a) The bar graph showing the percent of germaria with the different numbers of GSCs (2-3 GSCs, 1 GSC or 0 GSC) in the genotype indicated with aging. **1**: *Wild-type*, **2**: *Hrp38 -/-*, **3**: *Parg+/-; hrp38-/-*, **4**: *UASp-Hrp38:RFP/Nos-Gal4; Hrp38-/-*, **5**: *UASp-DE-cadherin/Nos-Gal4; Hrp38-/-*, **6**: *Parg+/-; UASp-Hrp38:RFP/Nos-Gal4; Hrp38-/-;* **7***: Parg+/-*; *UASp-DE-cadherin/Nos-Gal4; Hrp38-/-.* The sample size was shown above each bar. * P<0.05; ** P<0.01; *** P<0.001, analyzed by *t*-test. **(b,c)** Expression of Hrp38:RFP rescued GSC self-renewal ability of the *hrp38* mutant. **(b)** Two GSCs (circled) still present in the 14-day-old *hrp38* mutant expressing Hrp38:RFP in GSCs by *nos-Gal4* driver. **(c)** DE-cadherin expression in the interface between GSCs and cap cells in the same fly as in **(b)**. **(d,e,f)** Expression of DE-cadherin rescued GSC self-renewal ability of the *hrp38* mutant. **(d)** Two GSCs (circled) still present in the 14-day-old *hrp38* mutant with expression of DE-cadherin in GSCs by the *nos-Gal4* driver. **(e,f)** DE-cadherin expression (circled) in the interface between GSCs and cap cells in the same fly as **(d)**.

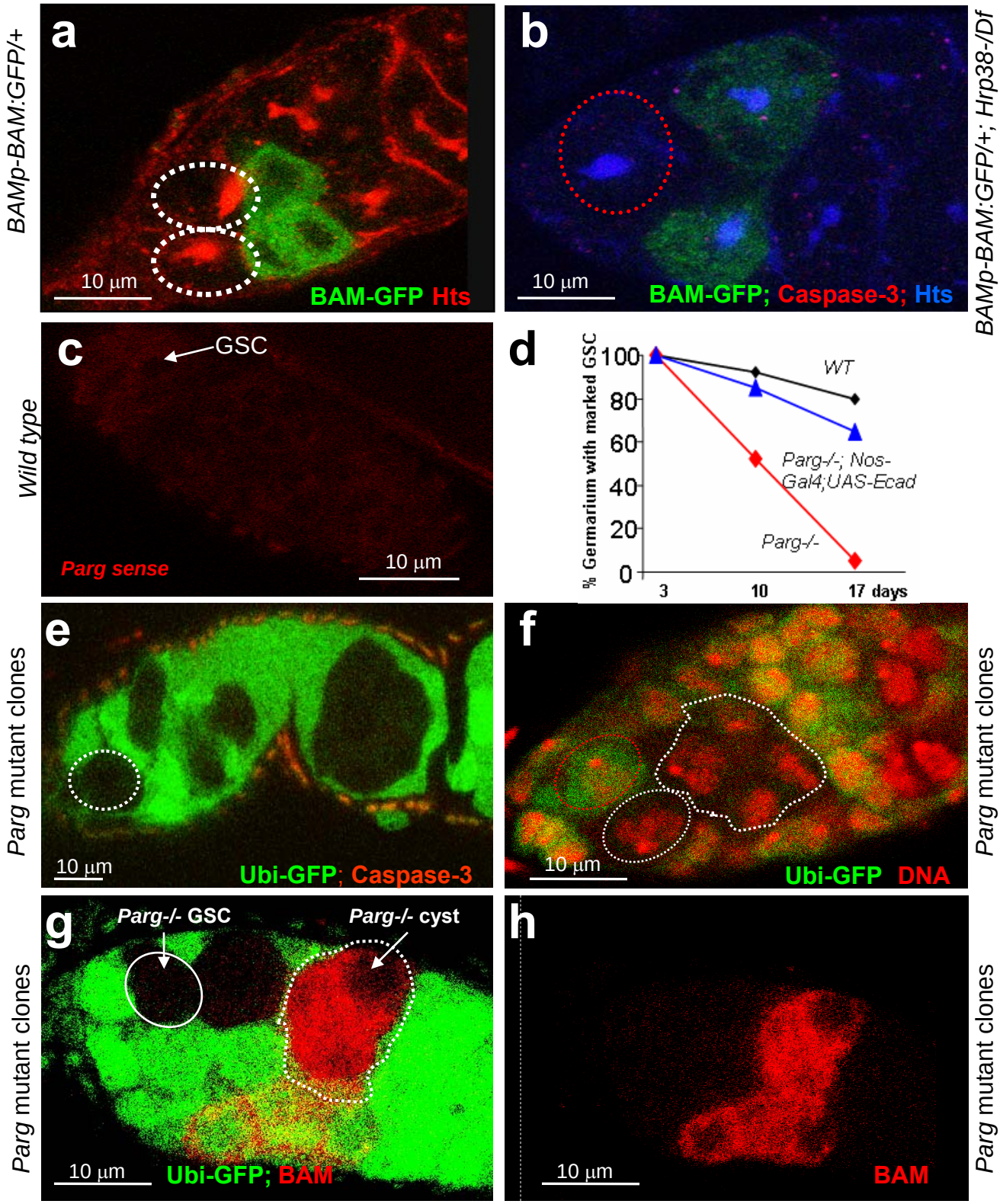

Supplementary Figure S5. BAM protein expresses normally in the *hrp38* and *Parg* mutants. **(a)** BAM-GFP expression in the cystoblast progeny in the 10-day-old BAM-GFP reporter line with two GSCs (circled). **(b)** BAM-GFP expression in the cystoblast progeny in the 10-day-old *hrp38* mutant with one GSC (circled). The same germarium was stained with anti-cleaved Caspase-3 antibody for detecting apoptosis. **(c)** The anti-sense control for *Parg* mRNA expression in GSC in the wild type (y,w) detected by RNA *in situ* hybridization. **(d)** The graph showing the percent of garmaria with marked GSCs with aging in different genotypes. *WT*: the wild-type fly with the wild-type marked GSC clones (*FRT101/ubi-GFP, FRT101; hs-FLP38/+*). *Parg-/-*: the fly carrying the *Parg* mutant GSC clones (*Parg27.1, FRT101/ubi-GFP, FRT101; hs-FL38/+*). *Parg-/-; Nos-Gal4; UAS-Ecad:* the fly carrying the *Parg* mutant GSC clones and DE-cadherin transgene (*Parg27.1, FRT101/ubi-GFP, FRT101; hs-FL38/Nos-Gal4; UASp>DE-cadherin/+).* **(e)** No apoptosis signals were detected in the germarium with *Parg* mutant GSC (circled) and its progeny one week after clone induction. Anti-cleaved Caspase-3 antibody was used for detecting apoptosis signals. **(f)** Intact DNA staining in the germarium with *Parg* mutant GSC (circled) and its progeny one week after clone induction. **(g,h)** BAM expression in the progeny of the *Parg* mutant GSC one week after clone induction.

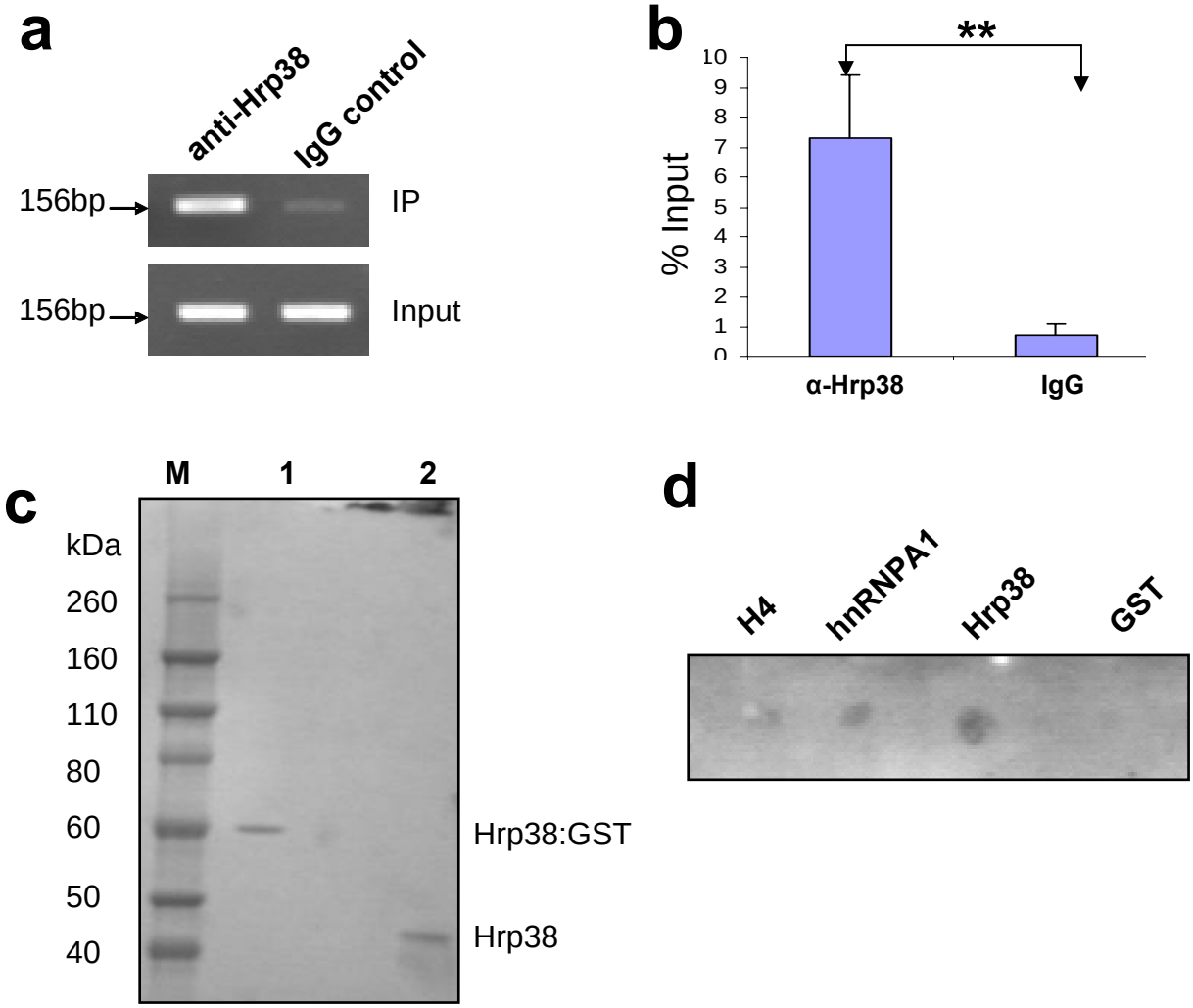

Supplementary Figure S6. Hrp38 protein interacts with DE-cadherin mRNA. (a, b) The association of Hrp38 with DE-cadherin mRNA in the wild-type ovary shown by regular RT-PCR **(a)** and qRT-PCR **(b)** after RNA-protein IP. RNA IP was carried out using anti-Hrp38 antibody and rabbit IgG as a control after formaldehyde cross-linking. The error bars representsthe standatd deviation from three independent experiments. ** P<0.01, analyzed by *t*-test. The error bar represents the standard deviation estimated based on three independent experiments. **(c)** Generation and purification of Hrp38 protein. 10 ng GST-Hrp38 recombinant protein (lane 1) or Hrp38 protein after cleaving of GST tag (lane 2) was resolved in SDS PAGE and stained with SimplyBlue Safe Stain to show the expected molecular weight. **(d)** Hrp38 binding to pADPr shown by dot-blot assay. 50 ng H4, GST-hnRNP A1, Hrp38 and GST were spotted in the membrane and incubated with 1ug/ml pADPr for one hour. pADPr binding to the proteins was detected with a rabbit anti-pADPr antibody.

Supplementary Table S1

Lethality caused by *Hrp38* mutations and RNAi

Parental genotypes	No. of progeny (progeny genotypes)		Percent lethality[a]
Hrp38^{d05172} / *TM6B (*F) x y,w (M)	268 (*Hrp38*^{d05172} /+)	178*(+/TM6B*)	
Df(3R)Exel^{6209}*/TM6B(F) x y,w(M)*	*262 (Df(3R)Exel*^{6209}*/+)*	155 *(+/TM6B*)	
Df(3R)Exel^{6209}*/TM6B(F) X Hrp38*$^{d05172/}$*TM6B (*M)	144(*Hrp38*^{d05172}*/ Df(3R)Exel*^{6209}*)*	*682 (-/TM6B)*	*75%*
Act5C-GAL4/CyO (F) X *y,w* (M)	200 (*Act5C*/+)	187(+/*CyO*)	
Act5C-GAL4/CyO (F) X *Hrp38-IR*^{29524} */CyO(M)*	0 (*Hrp38-IR*^{29524}*/Act5C-GAL4*)	292(+/CyO)	100%
Act5C-GAL4/CyO (F) X *Hrp38-IR*^{29523}*(M)*	84 (*Hrp38-IR*^{29523}*/Act5C-GAL4*,**F**)	208(+/CyO)	60%
y,w(F) X *TubP-GAL4/TM3,Sb* (M)	190 (*TubP-GAL4*/+)	122(+/*TM3,Sb*)	
Hrp38-IR29523 (F) X TubP-GAL4/TM3,Sb (M)	0 (*Hrp38-IR29523*/*TubP-GAL4*/+)	202(+/*TM3,Sb*)	100%

a: Percentage of lethality = [expected number– observed number)/expected number] x 100%. Expected numbers were normalized to the progeny of parallel crosses between *hrp38* mutation strains and *yw* strain.

Supplementary Table S2

Lethality of *hrp38* hemizygotes rescued by expression of UAST-Hrp38:RFP transgene

Parental genotypes:	arm-Gal4/Cyo; *Df(3R)Exel*^{6209}*/TM6B(F) X UAST-hrp38:RFP; Hrp38*^{d05172}*TM6B (M)*
Progeny genotypes (No. of Progeny)*:*	*arm-Gal4/UAST-hrp38:RFP; hrp38-/TM6B* (374)[a]
	UAST-hrp38:RFP/Cyo; hrp38-/TM6B (280)[a]
	UAST-hrp38:RFP/Cyo; Hrp38^{d05172}*/ Df(3R)Exel*^{6209} (36) (73% lethality*)*
	arm-Gal4/UAST-hrp38:RFP;Hrp38^{d05172}*/ Df(3R)Exel*^{6209} (202*)* (no lethality*)*

a: *; hrp38-/TM6B* includes both *hrp38* ^{d05172} */TM6B* and *Df(3R)Exel*^{6209} */TM6B* flies.

SUPPLEMENTARY DISCUSSION

Our findings that association between pADPr and a heterogeneous nuclear ribonucleoprotein Hrp38 controls DE-cadherin expression in the Drosophila ovary and thereby regulates egg chamber polarity and GSC maintenance has a number of interesting implications.

Fear of intimacy (FOI), a zinc transporter, has been shown to regulate DE-cadherin expression at the post-transcriptional level in the gonad (49). The authors of this study suggested that FOI could influence the activity of an RNA-binding protein with Zn availability for DE-cadherin expression. Therefore, it will be important to investigate whether the FOI mutant affects the activity of Hrp38 binding to 5' UTR of DE-cadherin. In addition, the lower penetrance of oocyte mislocalization in the *hrp38* mutant suggests that other hnRNP proteins may also contribute to upregulating *DE-cadherin* expression in the oocyte as IRES-mediated transacting factors. Indeed, a recent study showed that Hrp38 interacts with other hnRNP proteins (*hrp36* and *glo*) during splicing control (50). Identifying other IRES-mediated transacting factors for *DE-cadhern* translational control during oogenesis will be pursued in the future study.

Furthermore, poly(ADP-ribosyl)ation may have additional roles for stem cell maintenance besides regulating DE-cadherin translation because dividing GSC appeared to have the elevated pADPr level in the anaphase-telophase during mitosis (Figure 1B-D). Indeed, pADPr is required for spindle assembly and structure (51), which is important for regulating asymmetric division of stem cell (52). Because *Parg* mutant GSCs already had the elevated pADPr, the role of pADPr for regulating spindle structure was likely masked in the *Parg* mutant GSC. Therefore, the further research on PARP1 mutant GSC, which should lose pADPr accumulation in dividing GSC, will shed a light to understand how pADPr regulates GSC division.

Previous research has linked the accumulation of pADPr in cells with cellular decision between DNA repair and cell death pathways (53). One of the caveats from our study is that elevated poly(ADP-ribose) level in cells does not necessarily cause cell death in the context of the physiological condition because knocking out *Parg* in a tissue-specific way, such as in GSCs, did not cause apoptosis. It is generally believed that NAD consumption in the *Parg* mutants or after PARP1 activation by DNA damage causes depletion of ATP and

subsequently induces cell death (54,55). However, we did not detect any apoptotic signals in the *Parg* mutant GSCs or their offspring. This observation implies that the cells undergoing extensive pADPr synthesis may have the ability to replenish their NAD pool to prevent cell death either in the cell-autonomous mechanism or by its neighboring wild-type cells in the *Parg* mosaic condition. Indeed, a recent study showed that *Parg*-null TS (embryonic trophoblast stem) cells, even using *in vitro* culture, recorded elevated cellular NAD levels after DNA damage (56). Further study explaining how the cell coordinates NAD metabolism for pADPr synthesis will facilitate understating how tumor cells having an elevated pADPr level, such as in ovarian cancer (57), can survive and proliferate inside human body.

SUPPLEMENTARY METHOD

Supplementary Method S1: RNA in situ hybridization in the ovary

For the detection of *Parg* mRNA in the ovary, DIG-labeled *Parg* RNA antisense and sense probes were produced using a DIG RNA labeling kit (SP6/T7) (Roche). The templates for DIG labeling were amplified by RT-PCR (Invitrogen) from the total ovary RNA of *y,w* strain. The primer sequences were as follows:

5' TCTGCAGCCCATAAAGACG 3' (forward)
5' TAATACGACTCACTATAGGGAGAGTTTGTCGACCT GAGC3' (T7+reverse) for *Parg* antisense probe;
5' TAATACGACTCACTATAGGGAGATCTGCAGCCCATAAAGACG 3' (T7+forward)
5' GTTTGTCGACGACCTGAGC 3' (reverse) for *Parg* sense probe.

RNA *in situ* hybridization in the ovary dissected from the wild type (*y,w*) was performed according to the published protocol (58). The hybridization signals for *Parg* mRNA were detected using anti-DIG antibody conjugated with rhodamine (Roche). All images were visualized using the Leica TCS-NT confocal microscope.

Supplementary Method S2: Western blotting and qRT-PCR

50 ug total protein from the appropriate genotypes of the wandering third-instar larvae were extracted and measured as described (59). The protein was subjected to immunoblotting. The blot was incubated with rabbit anti-Hrp38 antibody at 1:10000 dilution

(a gift from Dr. J. A. Steitz) (60), mouse anti-Hrp36 antibody at 1:25 dilution (a gift from Dr. H. Saumweber) and rat anti-DE-cadherin antibody at 1:20 dilution (DCAD1, a gift from Dr. Takeichi) (61) as the primary antibodies. The signals were detected with horseradish peroxidase-conjugated secondary antiserum and ECL™ reagents (GE Health). The blots were stripped and detected with mouse anti-α-tubulin antibody at 1:1000 dilution (DM1A, Sigma) or mouse anti-actin antibody at 1:1000 dilution (MAB1501, Chemicon). All immuoblotting was repeated three times; the signal intensity was measured using Image J software (NIH). The mRNA expression level of DE-cadherin was measured by qRT-PCR based on the method described previously (59). The primer sequences for DE-cadherin were as follows: 5′ GACGAATCCATGTCGGAAAA 3′ (forward) and 5′ GATAATACCCGACTCCTTGTCAATC 3′ (reverse).

Supplementary Method S3: RNA–protein co-immunoprecipitation *in vivo*

Either 50 pairs of the wild-type ovaries or 3X 10^6 *Drosophila* S2 cells after a 24-hour transfection with *DE-cadherin* 5'UTR luciferase plasmid were treated with 1% formaldehyde in 1X PBS for 10 minutes. The reaction was stopped with 0.25M glycine for 5 minutes. After washing with 1X PBS, the ovaries or S2 cells were treated with the lysis buffer and IPed with rabbit anti-Hrp38 antibody (1:50) or IgG control (1:50) as described (59). IP complex was further treated with 0.2 mg/ ml proteinase K (Invitrogen) for 30 min at 50°C, followed with 1-hour incubation in 0.2 M NaCl at 65°C for reversing crosslink. RNA was further precipitated with Trizol (Invitrogen) and purified with RNeasy mini kit (Qiagen) after DNAase treatment. The real-time RT-PCR assay was done as described before (59) and repeated three times, beginning with IP. The primers for detecting DE-cadherin mRNA after the ovary IP were described as above for the quantitation of *DE-cadherin* expression in the larval stage. The primers for detecting *DE-cadherin* 5'UTR-luciferse transcript after S2 cell IP were as follows: 5′ GTGTGAGTGAAATAATACTGGGTGA 3′ (forward from DE-cadherin 5'UTR) and 5′ CTGTAAAAGCAATTGTTCCAGG 3′ (reverse from the firefly luciferase gene).

SUPPLEMENTARY REFERENCES

49. Mathews, W.R., Ong, D., Milutinovich, A.B., and Van Doren, M. Zinc transport activity of Fear of Intimacy is essential for proper gonad morphogenesis and DE-cadherin expression. Development **133**:1143-1153 (2006).

50. Guruharsha, K.G. and *et al.* A Protein Complex Network of Drosophila melanogaster. Cell **147:** 690-703 (2011).

51. Chang, P., Jacobson, M.K. and Mitchison, T.J. Poly(ADP-ribose) is required for spindle assembly and structure. Nature **432**, 645-449 (2004).

52. Cheng, J., Tiyaboonchai, A., Yamashita, Y.M. and Hunt, A.J. Asymmetric division of cyst stem cells in Drosophila testis is ensured by anaphase spindle repositioning. Development **138**,831-837 (2011).

53. D'Amours, D., Desnoyers, S., Silva, D. and Poirier, G. G. Poly(ADP-ribosyl)ation reactions in the regulation of nuclear functions. Biochem. J. **342**,249-268 (1999).

54. Koh, D.W., and *et al*. Failure to degrade poly(ADP-ribose) causes increased sensitivity to cytotoxicity and early embryonic lethality. PNAS **101**,17699-17704 (2004).

55. Amé J,C., and et al. Radiation-induced mitotic catastrophe in PARG-deficient cells. Journal of Cell Science **122**,1990-2002 (2009).

56. Zhou, Y., Feng, X. and Koh, D.W. Activation of Cell Death Mediated by Apoptosis-Inducing Factor Due to the Absence of Poly(ADP-ribose) Glycohydrolase. Biochemistry **50**, 2850-2859 (2011).

57. Fong, P. C. *et al*. Inhibition of poly(ADP-ribose) polymerase in tumors from BRCA mutation carriers. N. Engl. J. Med. **361**, 123–134 (2009).

58. Vanzo, N.F., and Ephrussi, A. Oskar anchoring restricts pole plasm formation to the posterior of the Drosophila oocyte. Development **129**, 3705-3714 (2002).

59. Ji, Y., and Tulin, A.V. Poly(ADP-ribosyl)ation of heterogeneous nuclear ribonucleoproteins modulates splicing. Nucl Acids Res **37,** 3501-3513 (2009).

60. Borah, S., Wong, A.C., and Steitz, J.A. Drosophila hnRNP A1 homologs Hrp36/Hrp38 enhance U2-type versus U12-type splicing to regulate alternative splicing of the prospero twintron. PNAS **106**, 2577-2582 (2009)

61. Oda, H., Uemura, T., Harada, Y., Iwai, Y., and Takeichi, M. A Drosophila Homolog of Cadherin Associated with Armadillo and Essential for Embryonic Cell-Cell Adhesion. Developmental Biology **165**, 716-726 (1994)